IOP Conf. Series: Materials Science and Engineering **724** (2020) 012017 doi:10.1088/1757-899X/724/1/012017

Tribological behaviour of sealing materials

C Birleanu[1], M Pustan[1], C Cosma[2], V Merie[3] and O Dranda[1]

[1]Mechanical Systems Engineering Department, Technical University of Cluj-Napoca, Cluj-Napoca, Romania
[2]Manufacturing Engineering Department, Technical University of Cluj-Napoca, Cluj-Napoca, Romania
[3]Materials Science and Engineering Department, Technical University of Cluj-Napoca, Cluj-Napoca, Romania

E-mail: Corina.Barleanu@omt.utcluj.ro

Abstract. The sealing elements are the most critical part of the mechanical sealing assembly and the main aspects of these are the tribological ones. The structural behaviour of the sealing components plays a crucial role in determining the sealing performance. Wide varieties of materials are used as seal face materials in practice. In this paper we focus on a couple of sealing materials CoCrWMo alloy / four different types of materials (copper-zinc alloy – brass, tin-copper alloy - bronze, graphite bronze and Teflon – PTFE). Dry and lubricant friction and ring on ring configuration are considered using a ring on ring tribometer. The rings from CoCrWMo alloy were additive manufactured using selective laser melting (SLM) process. Tribological tests were run at room temperature on different couples. These materials present different tribological behaviours in terms of sliding wear evaluation.

1. Introduction

Seals are used on a very large scale with direct influence on the reliability of mechanical systems (pumps, compressors, turbines, etc.). A dynamic seal is a mechanical device used to prevent liquid leakage when there is rotational movement between the sealing surfaces. In general, a mechanical seal works with an extremely thin film lubricant in the sealing space, the thickness thereof being typically in the range of 0.1-1.0 μm to reduce leakage and to limit friction and wear [1-3].

The best sealing materials have a low friction, high hardness differences, are not soluble in one another, good corrosion resistance, good bearing properties, good machining capacity and high thermal conductivity [4, 5].

Most dynamic seals, such as mechanical seals, fall into the category where friction surfaces are separated and lubricated with a thin film of lubricant [1]. Typical properties used for description of bulk material strength and deformation do not apply for thin films and micro devices. This size effect relationship is not yet well understood when structural dimensions decrease from millimeters to micro and nanometers [1].

A schematic presentation of a conventional mechanical face seal is presented in figure 1. Mechanical face seals mainly contain two rings adjusted on the rotating shaft. One part (face) is a rotating ring that is attached to the shaft and rotates with it and the other is stationary and is mounted in the housing. The rotating face can move along the shaft axis allowing relative movement and provide flexibility for small misalignment between the parts.

Content from this work may be used under the terms of the Creative Commons Attribution 3.0 licence. Any further distribution of this work must maintain attribution to the author(s) and the title of the work, journal citation and DOI.
Published under licence by IOP Publishing Ltd

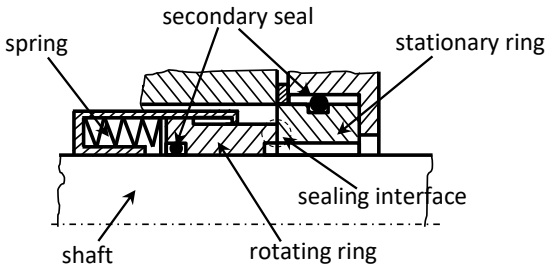

Figure 1. Schematic presentation of a mechanical face seal as a tribosystem.

We specified that the purpose of tribological studies in this paper is to establish a scientific approach to predict the friction state of mechanical seals based on higher material performance. CoCrWMo alloy widely used as a hard material is a potential candidate for but its tribomechanical properties need to be investigated in the aim of used in high performance mechanical seal working in severe conditions. CoCrWMo alloy offers good mechanical properties (hardness, Young modulus), resistance to corrosion and thermal conductivity that make it proper for tribological application in dry and lubricated sliding. Combined with matting face ring from a softer material, the sliding of CoCrWMo alloy can be sustained in severe working conditions [6].

In this paper the experimental investigations assesses the tribological behaviors of CoCrWMo alloy against four different sealing materials

2. Experimental procedures

2.1. Sample materials

The active semi-ring from the friction coupler made from CoCrWMo (commercially named Starbond CoS55) alloy was manufactured by selective laser melting (SLM) process. SLM is a complex thermo-physical process that largely depends on material, laser and process parameters (Figure 2). The main component is the solid Nd:YAG laser which emits continuous light with a wavelength of 1064 nm in infra-red spectrum. The system used was Realizer SLM 250 (Germany) and 50 μm the value of spot laser. The following SLM parameters could be set up on Realizer equipment: 20-200 W laser power, 20-100 μm layer thickness, 100-2000 mm/s scanning speed, 0.06-0.20mm hatch space and various scanning strategies (eq. X/Y, stripe hatch pattern, islands).

Two rings made of CoCrWMo alloy provided by Scheftner, Germany were manufactured by SLM (selective laser melting). This alloy is highly corrosion resistant and has a density of about 8.8 g/cm^3. The solidus-liquidus interval of it is between 1305-1400 ºC. The mass percentages of each chemical element are presented in Table 1. The diameter of CoCr grains is between 10-55 μm and they are spherical.

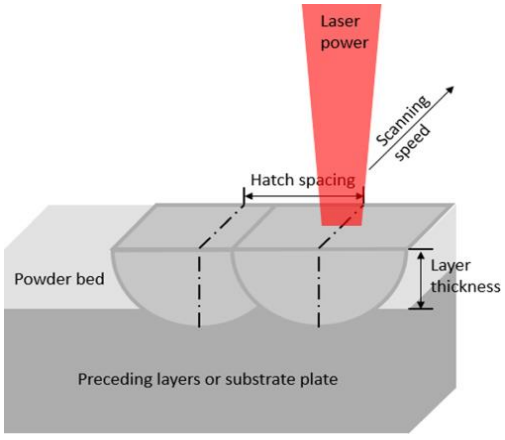

Figure 2. The main SLM process parameter [7].

Table 1. Chemical composition of the CoCrWMo powder.

Chemical element	Co	Cr	W	Mo	Si	Other elements (C, Fe, Mn, N)
Maximum weight percentage [%]	59	25	9.5	3.5	1	< 1

In order to avoid the unfavourable effects of residual stress, after SLM manufacturing the parts were exposed on a thermal treatment. This heat treatment was performed in an electric oven and air atmosphere. The parts were heated up to 860 °C with 7 °C/min. At this temperature the parts were hold for 1h and followed by cooling rate of 12°C/min. After the temperature decrease to 300 °C, we open the door of furnace for natural cooling. In the end, the parts were sandblasted with alumina. To archive the required accuracy, the rings were conventional processed (CNC turning).

Normally, after conventional manufacturing such as casting, the hardness of this CoCr alloy is between 407-601 HV1 [8]. Based on our previously research, the hardness of parts SLM processed is directly influenced by process parameters such as laser power, scanning speed or by the density of energy which is distributed on each powder slice [9]. Due to this know-how, its need to determine also the hardness obtained on rings manufactured with the following SLM conditions.

The dimensions for the primary ring from CoCrWMo are 62 mm for external diameter, D, and 4 mm thickness of hardness 540 HV1 (51,8 HRC). For the second ring (soft sample) diameter is 16 mm and 6 mm thickness and four different materials with a surface hardness presented in table 2. In the paper were defined as soft samples as follows: sample 1 made from copper-zinc alloy named brass (CuZn40PtSn); sample 2 from tin-copper alloy named bronze (BzA15), sample 3 from graphite bronze and sample 4 from teflon – PTFE.

The hardness values (table 2) are the average of 12-15 determinations per sample. The hardness was evaluated using a Microhardness Tester VMHT with the trace marks shown in figure 3.

Table 2. Rings hardness values.

Rings material	CoCrWMo primary ring	Material for soft samples			
		Sample 1	Sample 2	Sample 3	Sample 4
Hardness HV0.5 (GPa)	5.4	1.906	1.634	0.460	0.033

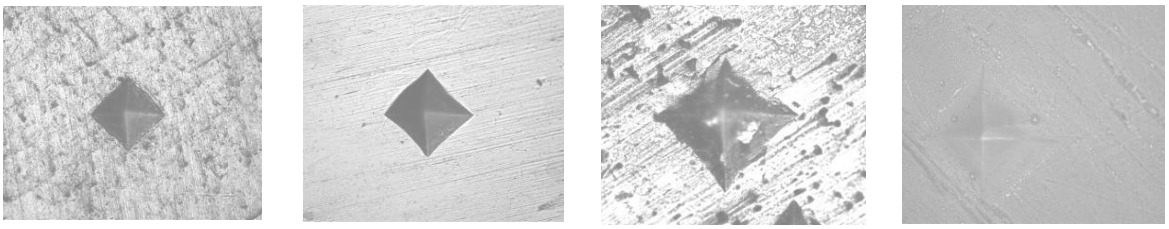

Sample 1 Sample 2 Sample 3 Sample 4

Figure 3. Indentation marks for the samples (soft samples).

2.2. Measurement of surface characteristics

Good surface roughness and flatness should be ensured to acquire low friction between seal faces. The surface of primary ring, SLM made from CoCrWMo alloy was polished to show an arithmetical mean height R_a less than 0.4 µm.

Four different sealing materials introduced above were selected as matting face rings. In the same way the surface were manufactured and R_a roughness for them is: sample 1 - 0.12 µm; sample 2 - 0.35 µm; sample 3 – 2.2 µm and sample 4 - 0.6 µm.

2.3. Tribometer and method

In this paper, we evaluated the sliding wear behaviours of a CoCrWMo alloy ring on four different materials rings in dry and lubricated environment using ring on ring tribometer in simulating the

sliding wear process of material couples (figure 4). The using rings on ring tests were performed in dry and lubricated environment respectively to investigate the effect of lubrication on the wear behaviour. The lubricated test was performed in the T80W90 mechanical transmission oil. The wear track was examined using ZEISS Smartzoom 5 smart digital microscope.

Figure 4. Friction test set-up for sample 4.

Loading the friction coupler is done by a lever system by mounting the weights on the two arms. The load that sits on the plates is $F_1 = 10$ N, and second test with $F_1 = 30$ N.

The normal load that loads the friction coupler is:

$$F_{n1} = F_1 \cdot \frac{c}{d} \cdot \frac{a}{a+d} = 72.64\ N \text{ and for second test } F_{n1} = 217.91\ N \quad (1)$$

Where a, b, c, d represents the tribometric lever system. The total normal load will consider the weight of the arms and plates which are producing an additional charge $F_{n2} = 10\ N$.

$$F_n = F_{n1} + F_{n2} = 82.64\ N \text{ and respectively, } F_n = 227.91\ N. \quad (2)$$

The speed at the vertical shaft is $n = 980$ rpm and the peripheral speed is:

$$v = \frac{\pi \cdot D \cdot n}{60 \cdot 1000} = 3.18\ m \cdot s^{-1}. \quad (3)$$

The wear rate, *W*, was evaluated using the formula $W = V \cdot (F_n \cdot s)^{-1}$ where *V* is the worn volume, F_n is the normal load, *s* is the sliding distance. The wear volume *V* is determined with both ZEISS Smartzoom 5 smart digital microscope and through the difference between the sample masses before and after wear $(m_0 - m_1)$ [g] using an accurate balance type Kern AEJ with a measurement accuracy of 0.1 mg.

The specimens were washed with diluent and dried and then weighed before and after the test.

The surface topography of worn rings was determined using an optical microscope. All measurements were done at room temperature (RT). The test time was *t* = 60 minutes means 11448 m sliding distance per test.

3. Results and discussions

The wear track volumes and wear rates are listed in Table 3 and Table 4 and were calculated based on the formulas above. The density was determined for each sample based on mass measurements and exact volume determination. The density values are shown in Table 3 and 4.

Table 3. Result summary of dry wear tracks measured using different test parameters (F_1 = 10 N, operating time = 60 s, ambient temperature).

	Wear Track height (μm)	Wear Volume (mm^3)	Wear Rate ($mm^3/N \cdot m$)
Sample 1 – ρ = 8.4515 g/cm^3	288.00	13.8082	0.8757 x 10^{-3}
Sample 2 – ρ = 8.2123 g/cm^3	202.30	25.0843	1.5908 x 10^{-3}
Sample 3 – ρ = 6.2206 g/cm^3	96.60	2.25058	0.1427 x 10^{-3}
Sample 4 – ρ = 2.1310 g/cm^3	373.00	44.2984	2.8094 x 10^{-3}

Table 4. Result summary of lubricated wear tracks measured using different test parameters (F_1 = 10 N / F_1 = 30 N, operating time = 3600 s, ambient temperature).

	Wear Track height (µm)	Wear Volume (mm^3)	Wear Rate ($mm^3/N{\cdot}m$)
Sample 1 – ρ = 8.4515 g/cm^3	49.10	0.07099	0.07503 x 10^{-6}
	84.20	0.13015	0.04988 x 10^{-6}
Sample 2 – ρ = 8.2123 g/cm^3	48.70	0.02435	0.02574 x 10^{-6}
	54.00	inconclusive result	inconclusive result
Sample 3 – ρ = 6.2206 g/cm^3	18.90	inconclusive result	inconclusive result
	25.70	inconclusive result	inconclusive result
Sample 4 – ρ = 2.1310 g/cm^3	56.20	0.6912	0.73 x 10^{-6}
	163.50	7.0858	2.7158 x 10^{-6}

The soft samples after the dry wear test exhibits a bigger wear scar of volume. As expected, the most pronounced wear is at sample 4 (PTFE) in the amount of ~44.3 mm^3 and the least is worn sample 3 of bronze graphite in value of ~2.25 mm^3. In comparison, the wear test carried out in the mineral oil lubricant creates a substantially smaller wear track with a volume of only ~0.69 mm^3 at sample 4 (PTFE) loaded with 10N and ~7.1 mm^3 loaded with 30 N, respectively.

Figure 5 and 6 shows the optical images of the wear scars on the soft samples (the first and the third samples) after the dry and lubricated wear tests, respectively. Optical microscopy analyses were performed in order to study the surface of the samples. The tests were carried out on an Olympus GX 51 microscope. All the samples were investigated at a magnification of 50:1. We can affirm that severe wear takes place during the Ring-on-Ring test in the dry atmosphere, compared to mild parallel wear scars on the samples after the much longer lubricated wear test. The high heat (around 80-90 ºC) and intense vibration generated during the dry wear test promotes oxidation of the metallic debris and results in severe three-body abrasion. We can observe in the case of dry testing that they were affected by the sudden rise in temperature in the contact area between the sample and the rotating ring (sometimes the temperature reached 90-100 ºC).

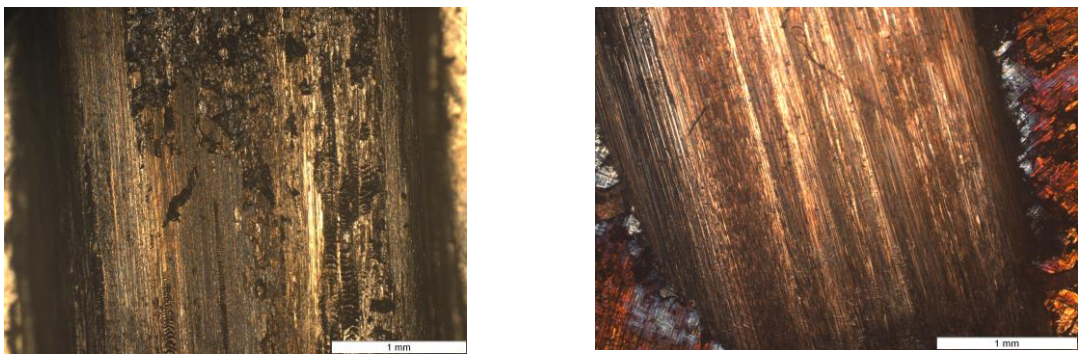

Sample 1 **Sample 3**

Figure 5. Wear scars of the soft samples after dry wear tests under 10 N applied force and 60 s operating time at RT for the first and the third samples, magnification of 50:1.

In the lubricated test, however, the mineral oil ultimately reduces the friction and cools the contact face, as well as transports away abrasive debris created during wear, leading to significant reduction of wear rate. It was found that for the graphite bronze due to the structure of the material it absorbed oil during the lubricated test and thus the volume of wear material could not be expressed by the mass difference. Therefore, these results were not convinced by this method. Such a substantial difference in wear resistance measured in different environment shows the importance of proper simulating sliding wear in the realistic service condition.

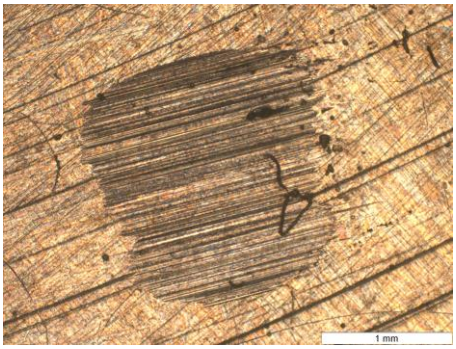

Sample 1

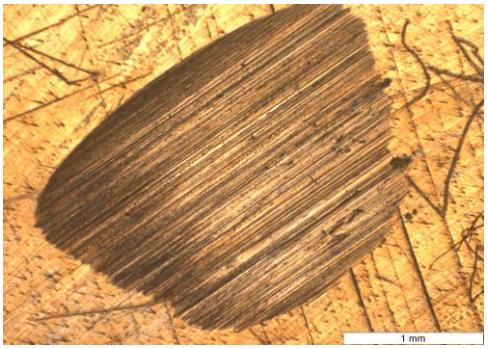

Sample 1

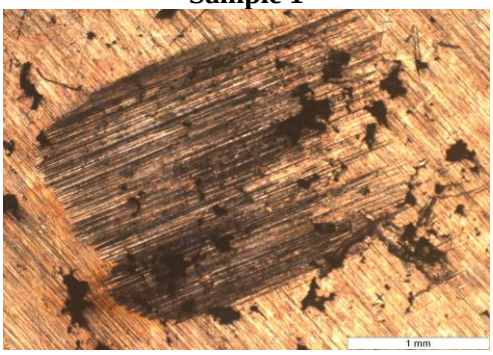

Sample 3

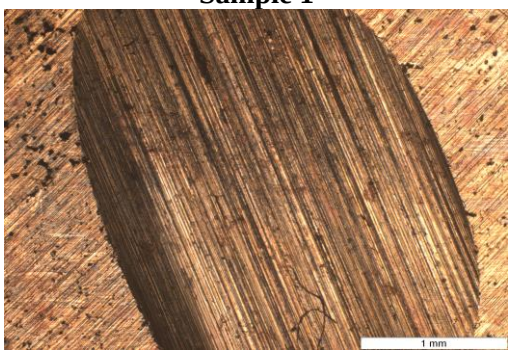

Sample 3

Figure 6. Wear scars of the soft samples after lubricated wear tests under 10 N and 30 N applied force and one-hour operating time and RT for the first and the third samples, magnification of 50:1.

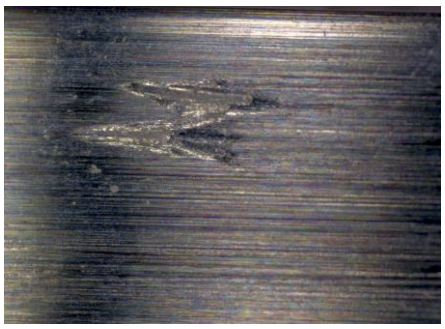

CoCrWMo ring surface after lubricated test (30 N)

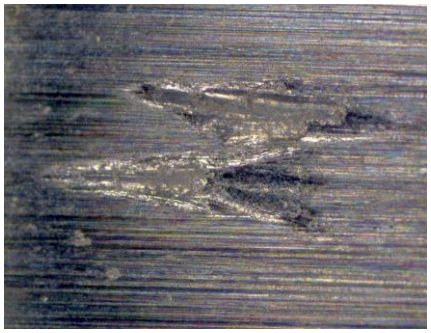

CoCrWMo ring surface after dry test (10 N)

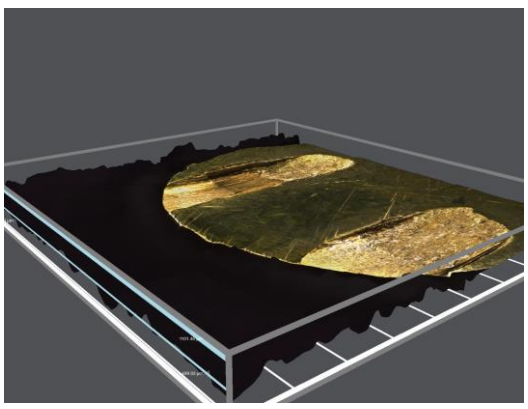

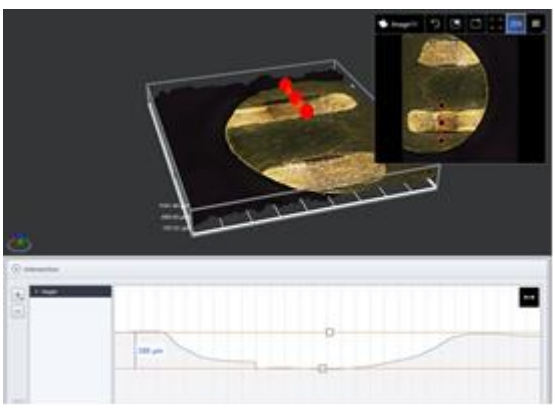

Samples 1 – surface images after dry test (10 N)

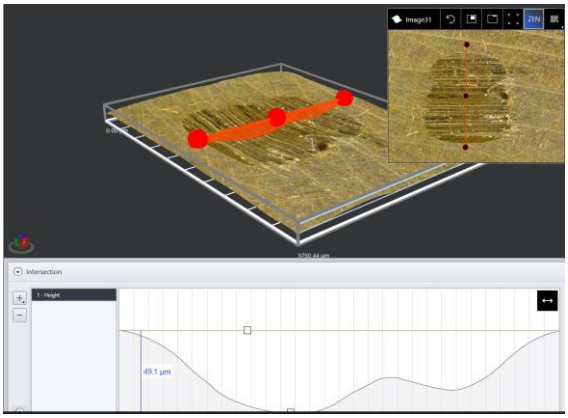

Samples 1 – surface images after lubricated test (10 N)

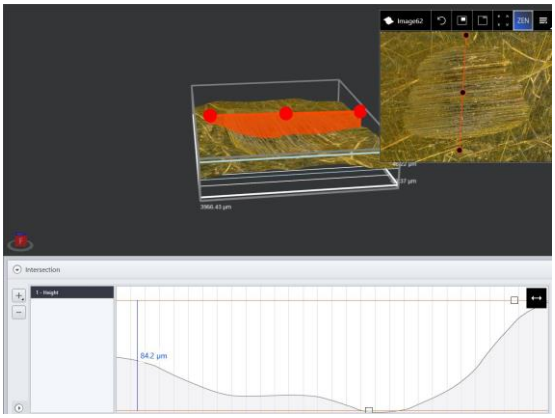

Samples 1 – surface images after lubricated test (30 N)

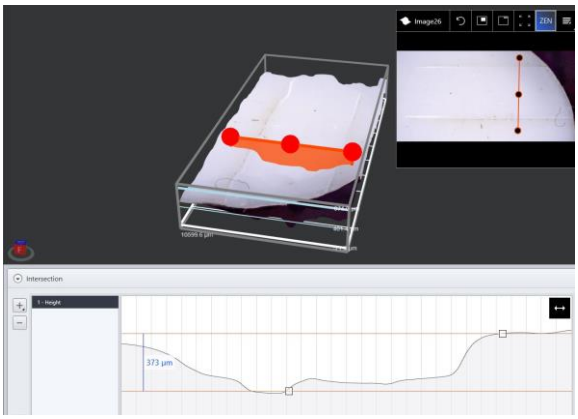

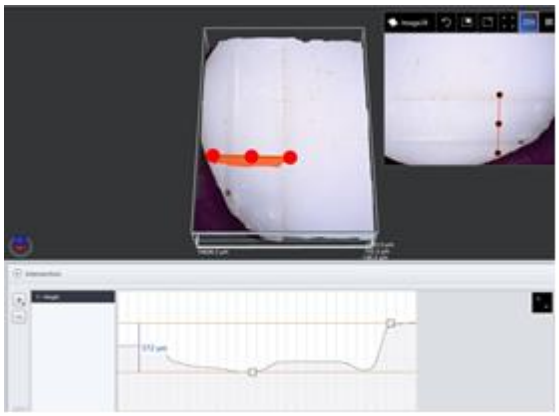

Samples 4 – surface images after dry test (10 N)

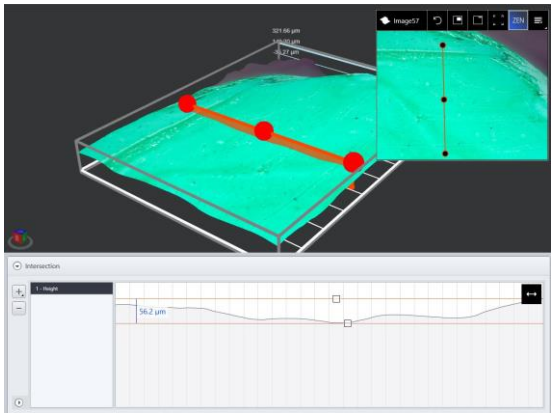

Samples 4 – surface images after lubricated test (10 N)

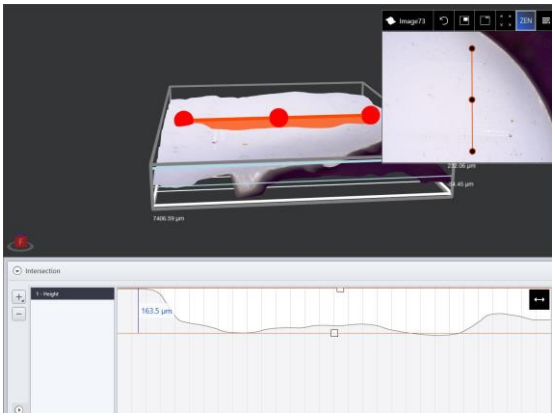

Samples 4 – surface images after lubricated test (30 N)

Figure 7. Wear scar profiles on the primary ring and soft samples for dry and lubricated wear tests.

The surface conditions of the CoCrWMo primarily ring and soft samples were examined by ZEISS Smartzoom 5 smart digital microscope. Figure 7 shows the surface morphology of the rings after the wear tests as an example. The four soft samples were analysed with this microscope under dry and lubricated conditions. In case of lubricant tests, two values for the force applied to the friction coupler were used 10 N and 30 N). All experimental results obtained on the wear track

depth are presented in Tables 3 and 4. Significant roughening of the surface took place due to the three-body abrasion process during the dry wear test of 980 revolutions.

Severe wear quickly damages the contact surface without lubrication and leads to irreversible deterioration of the surface quality. Wear rate values for both primarily ring and soft samples are calculated from the volume of material lost during a specific friction run. The primarily ring scar depth is measured to calculate the ring scar volume, and soft samples scar volumes are calculated from samples weight loss. This simple method facilitates the determination and study of wear behaviour of almost every solid-state material combination, with varying time, contact pressure, velocity, temperature, humidity, lubrication, etc.

4. Conclusions

A higher wear loss is observed from the dry sliding test for CoCrWMo alloy/graphite bronze during a running-in period and accommodation. A third body is created mainly from the wear of the sealing materials ring. The impregnation of the graphite material plays a predominate role in the tribological performance of the matting face material. This third body acts like a solid lubricant reduces the stick-slip phenomenon inside the contact. A better resistance to the wear is achieved with these pairs of materials. The contact accommodations provide the best behaviour in terms of friction and then reduce also the mechanical vibrations and the noises.

In all cases, the surfaces of the friction pair are covered with oxides and adsorbed gases that fundamentally change the surface friction properties. The presence of the oxide layer is the result of a dynamic process of forming on one side and wear on the other. As it is different from static oxidation, oxidation of the friction surface is stimulated by both high temperature and surface activation and is the result of the friction process, more evident in dry friction.

When sealing rings connect each other, the tribological characteristics of the material combination determine the survival or failure of the seal. The best material used for sealing couplings have low friction, high hardness differences are not soluble with each other, have good corrosion resistance, good processing ability and high thermal conductivity.

In conclusion, based on the experimental experiments performed, we appreciate that in contact with the proposed CoCrWMo alloy material as the sealing friction semi coupling the mate material with the best tribological behaviour under both dry and lubricated conditions is graphite bronze. At lower loads it is not to be neglected either the CoCrWMo alloy material coupling with PTFE.

5. References

[1] Towsyfyan H 2017 Investigation of the Nonlinear Tribological Behaviour of Mechanical Seals for Online Condition Monitoring, Doctoral thesis, University of Huddersfield.
[2] Nau B 1997 *Proc. Inst. Mech. Eng. J: J. Eng. Tribol.* **211(3)** 165.
[3] Minet C, Brunetière N and Tournerie B 2012 *Proc. Inst. Mech. Eng. J: J. Eng. Tribol.* **226 (12)** p. 1109-1126
[4] Pustan M 2006 Contribuţii privind etanşările frontale cu impulsuri, Doctoral Thesis, Technical University of Cluj-Napoca
[5] Birleanu C and Sucala F 2008 *Tribol. Ind.* **30** 10.
[6] Zaidi H and Paulmier A 1991 *Surf. Sci.* **251** 778.
[7] Yap C Y, Chua C. K et all 2015 Review of selective laser melting: Materials and applications, Applied Physics Reviews **2**
[8] Young W C and Budynas R G 2002 *Roark's formulas for stress and strain* **7** (New York: McGraw-Hill).
[9] Cosma C, Balc N, Moldovan M, Morovic L, Gogola P and Borzan C 2017 *J. Optoelectron. Adv. Mater.* **19 (11-12)** 738.